Kinetic and Chemical Mechanisms of the *fabG*-Encoded *Streptococcus pneumoniae* β-Ketoacyl-ACP Reductase

Mehul P. Patel,[‡] Wu-Schyong Liu,[§] Joshua West,[||] David Tew,[‡] Thomas D. Meek,*[,‡] and Sara H. Thrall[‡]

Assay Development, Discovery Research, Gene Expression and Protein Biochemistry, Discovery Research, and Microbial, Musculoskeletal and Proliferative Diseases Center of Excellence of Drug Discovery, GlaxoSmithKline Pharmaceuticals, 1250 South Collegeville Road, Collegeville, Pennsylvania 19426-0989

Received May 23, 2005; Revised Manuscript Received September 8, 2005

ABSTRACT: β-Ketoacyl-acyl carrier protein reductase (KACPR) catalyzes the NADPH-dependent reduction of β-ketoacyl-acyl carrier protein (AcAc-ACP) to generate (3*S*)-β-hydroxyacyl-ACP during the chain-elongation reaction of bacterial fatty acid biosynthesis. We report the evaluation of the kinetic and chemical mechanisms of KACPR using acetoacetyl-CoA (AcAc-CoA) as a substrate. Initial velocity, product inhibition, and deuterium kinetic isotope effect studies were consistent with a random bi-bi rapid-equilibrium kinetic mechanism of KACPR with formation of an enzyme-$NADP^+$−AcAc-CoA dead-end complex. Plots of log V/K_{NADPH} and log $V/K_{AcAc-CoA}$ indicated the presence of a single basic group (pK = 5.0−5.8) and a single acidic group (pK = 8.0−8.8) involved in catalysis, while the plot of log V vs pH indicated that at high pH an unprotonated form of the ternary enzyme complex was able to undergo catalysis. Significant and identical primary deuterium kinetic isotope effects were observed for V (2.6 ± 0.4), V/K_{NADPH} (2.6 ± 0.1), and $V/K_{AcAc-CoA}$ (2.6 ± 0.1) at pH 7.6, but all three values attenuated to values of near unity (1.1 ± 0.03 or 0.91 ± 0.02) at pH 10. Similarly, the large α-secondary deuterium kinetic isotope effect of 1.15 ± 0.02 observed for [4*R*-^{2}H]NADPH on $V/K_{AcAc-CoA}$ at pH 7.6 was reduced to a value of unity (1.00 ± 0.04) at high pH. The complete analysis of the pH profiles and the solvent, primary, secondary, and multiple deuterium isotope effects were most consistent with a chemical mechanism of KACPR that is stepwise, wherein the hydride-transfer step is followed by protonation of the enolate intermediate. Estimations of the intrinsic primary and secondary deuterium isotope effects (^Dk = 2.7, $^{\alpha-D}k$ = 1.16) and the correspondingly negligible commitment factors suggest a nearly full expression of the intrinsic isotope effects on $^DV/K$ and $^{\alpha-D}V/K$, and are consistent with a late transition state for the hydride transfer step. Conversely, the estimated intrinsic solvent effect (^{D_2O}k) of 5.3 was poorly expressed in the experimentally derived parameters $^{D_2O}V/K$ and ^{D_2O}V (both = 1.2 ± 0.1), in agreement with the estimation that the catalytic commitment factor for proton transfer to the enolate intermediate is large. Such detailed knowledge of the chemical mechanism of KAPCR may now help guide the rational design of, or inform screening assay-design strategies for, potent inhibitors of this and related enzymes of the short chain dehydrogenase enzyme class.

Streptococcus pneumoniae is a leading cause of respiratory infections in children, the elderly, and persons with chronic medical conditions that result in a compromised immune system. The emergence of multidrug-resistant pneumococcal bacteria has diluted the effectiveness of current antibiotic therapies, resulting in an urgent need for novel antimicrobial agents that target different metabolic pathways than do current therapies. Fatty acid biosynthesis is essential to the survival of bacteria, and its associated enzymes thereby comprise exploitable drug-discovery targets, especially in view of the differences between fatty acid biosynthesis in prokaryotes (FAS I) and mammals (FAS II) (*2*). The genes encoding the enzymes involved in fatty acid biosynthesis have been identified from several bacterial genomes (*3*). The *fabG*-encoded β-ketoacyl-ACP reductase (KACPR[1]) (EC 1.1.1.100) catalyzes the only known keto-acid reductase in bacterial fatty acid biosynthesis, making this enzyme an ideal target for the development of novel antibiotic drugs (*3*−*5*). To date, however, the only KACPR inhibitors reported are weak, undevelopable, plant-derived polyphenols (*6*). KACPR catalyzes the NADPH-dependent reduction of β-ketoacyl-ACP, the product of the β-ketoacyl-ACP synthase condensing enzymes. The β-hydroxyl-acyl-ACP product of the KACPR reaction is subsequently dehydrated, and reduced to form a saturated alkyl chain that undergoes repeated cycles of elongation until the physiologically optimal chain length is obtained (Scheme 1).

KACPR belongs to the family of short-chain dehydrogenases/reductases (SDR) (*7*). Although only 15−30% se-

* Corresponding author. Phone: (610) 917 6786. Fax: (610) 917 7379. E-mail: Thomas_Meek-1@gsk.com.

[‡] Assay Development, Discovery Research.

[§] Gene Expression and Protein Biochemistry, Discovery Research.

[||] Microbial, Musculoskeletal and Proliferative Diseases Center of Excellence of Drug Discovery.

[1] Abbreviations: KACPR, β-ketoacyl-ACP reductase; AcAc-ACP, acetoacetyl-acyl carrier protein; AcAc-CoA, acetoacetyl-Coenzyme A; Hepes, 4-(2-hydroxyethyl)-1-piperazineethanesulfonic acid; β-NADPH, reduced β-nicotinamide adenine dinucleotide phosphate.

10.1021/bi050947j CCC: $30.25
Published on Web 11/22/2005

Scheme 1: *S. pneumoniae* Fatty Acid Biosynthesis

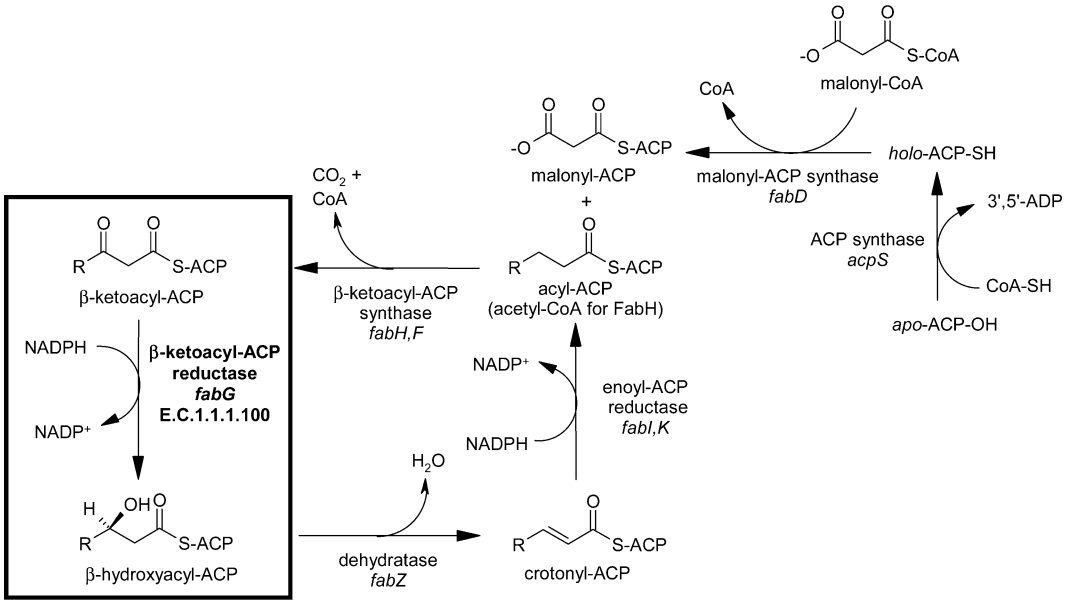

quence identity exists between the roughly 300 different SDR enzymes, sequence, structural, and directed mutagenesis comparisons of all members of this family of enzymes have revealed a strong conservation of α/β protein folding patterns consistent with a Rossman-fold, and the participation of a Ser-Tyr-Lys active site triad in a catalytically essential proton relay system (*7*). Structural studies of KAPCR from *Escherichia coli*, *Brassica napus*, and *Mycobacterium tuberculosis* confirmed the presence of the active site triad, and in the case of *E. coli*, a proton network (*8*−*10*). The structural studies of KACPR from *E. coli* with $NADP^+$ or NADPH bound suggested that NADPH binding promotes the formation of the conserved proton network formed between the side chains of the active site Ser-Tyr-Lys triad, several solvent molecules, and the cofactor ribose hydroxyl groups (*11*). The authors proposed that the function of this proton−water network is to align active site residues for catalysis, and to allow replenishment from solvent of the proton delivered from Tyr151 to substrate (AcAc-ACP) after catalysis. Although no structure exists for AcAc-CoA or AcAc-ACP bound to KACPR, the structural data also provided evidence for substantial conformational changes induced by binding of cofactor NADPH, from which these authors inferred an ordered kinetic mechanism of KACPR wherein NADPH binding induces a conformation of the enzyme that is essential for AcAc-ACP to bind. In fact, a recent review of type II fatty acid synthesis reported that KACPR catalysis proceeds via a compulsory-ordered mechanism in which the binding of the cofactor must precede substrate binding (*3*). Yet no studies to date have reported on the elucidation of the kinetic and chemical mechanism of KACPR. This knowledge would appropriately complement the structural data to reveal the actual catalytic mechanism of KACPR.

Steady-state kinetics, pH, and kinetic isotope effect studies were used to characterize the kinetic and chemical mechanisms of *S. pneumoniae* β-ketoacyl-ACP reductase. In addition to providing starting points for the rational design of potent KACPR inhibitors, the in-depth understanding of the catalytic steps of KACPR, including characterization of the reaction transition states revealed by this work, may also provide a general model for other short chain dehydrogenase enzymes, which can begin to have impact on other drug-discovery efforts for diseases wherein SDRs play a role.

EXPERIMENTAL PROCEDURES

Materials. Acetoacetyl-CoA, NADPH, $NADP^+$, D-[1-^{2}H]-Glucose (97 atom % ^{2}H), ethanol-d_6, *Leuconostoc mesenteroides* (type XXIV) glucose-6-phosphate dehydrogenase, *Leuconostoc mesenteroides* alcohol dehydrogenase, *Leuconostoc mesenteroides* aldehyde dehydrogenase, yeast hexokinase, ATP, methylamine, ethylamine, propylamine, and all buffers were purchased from Sigma. Deuterated water (D_2O) was purchased from Cambridge Isotope Laboratories 99.9 atom % ^{2}H. *Pwo* polymerase and Complete protease inhibitor cocktail was purchased from Roche Biochemicals. IPTG, *Dpn*I, and dNTPs were obtained from Invitrogen; HiTrap columns used for purification of KACPR were purchased from Amersham Pharmacia Biotech.

Preparation of Deuterated NADPH. [4*S*-^{2}H] NADPH and [4*R*-^{2}H] NADPH were enzymatically synthesized as previously described by Orr and Blanchard and Morrison and Stone, respectively (*12*, *13*) The purification of [4*S*-^{2}H]-NADPH and [4*R*-^{2}H]NADPH was performed using a MonoQ column, and fractions with absorbance ratios $A_{260}/A_{340} \leq 2.3$ were pooled, as previously described (*12*). The pooled fractions were freeze-dried and stored at −70 °C. The concentration of the purified, reduced nucleotides was determined by enzymatic end-point assays using glutathione reductase with excess glutathione disulfide. Purified, recombinant AcAc-ACP from *E. coli* was a gift from Dr. Howard Kallender and John Martin (GlaxoSmithKline Pharmaceuticals).

Cloning, Expression, and Purification of KACPR. The *fabG* gene, encoding β-ketoacyl-ACP reductase, was obtained by PCR amplification of the gene from genomic DNA of *S. pneumoniae* strain 0100993 using *Pwo* polymerase with the following primers: 5′-GGCGCTTACATATGAAACT-AGAACATAAAAAT-3′ (forward primer) and 5′-CTAGG-

ATCCCGCTACATACTTAAGCCACCA-3′ (reverse primer). The amplified gene product was cloned into the *E. coli* expression vector pET24b(+) (Novagen, Madison, WI) at the *Nde*I and *Bam*HI sites to create pET24bSpFabG. The plasmid construct was transformed into *E. coli* BL21 (DE3) cells for expression. An overnight culture was grown in LB medium containing 50 μg/mL kanamycin and 1% glucose, diluted 1:100 and grown at 37 °C to an absorbance at OD_{600} of ∼0.6. IPTG (0.5 mM) was added to the culture, and growth was continued for an additional 3 h at 37 °C. Cells were harvested and suspended in 50 mM Tris pH 7.5, 1 mM EDTA, 2 mM DTT, and Complete protease inhibitor cocktail at a volume of 5 mL/g of cells. Lysis was carried out using lysozyme treatment followed by 3 cycles of sonication, freezing, and thawing. Clarified lysate was applied to a 5 mL HiTrap Blue Sepharose column and eluted with a 100 mL gradient from 0 to 1 M NaCl in the above buffer without protease inhibitors. Fractions were analyzed by SDS−PAGE and by measurement of KACPR activity, and those fractions containing KACPR activity were pooled and precipitated with 80% $(NH_4)_2SO_4$. Pellets were dissolved in 50 mM Tris pH 7.5, and dialyzed overnight at 4 °C against the same buffer. Samples were applied to a 5 mL HiTrap Q column and eluted with a 100 mL, 0−1 M NaCl (in 50 mM Tris pH 7.5) linear gradient. Fractions containing KACPR activity were pooled and dialyzed against 50 mM Tris pH 7.0, 0.1 M NaCl, 50% glycerol, and stored at −20 °C. Amino-terminal sequencing, MALDI-MS, and amino acid analysis were performed on the purified sample to confirm the identity of the protein.

Steady-State Kinetics. Initial rates of the KACPR reaction using either β-acetoacetyl-CoA or acetoacetyl-ACP as substrates were measured by monitoring the decrease in absorbance of NADPH at 340 or 370 nm at 30 °C in 96-well half-area clear bottom plates (Corning) using a 96-well plate spectrophotometer (SpectraMax, Molecular Devices). Assays were performed in 50 mM HEPES (pH 7.6), 100 mM NaCl, and 15 nM KACPR, in total volumes of either 50 or 100 μL. The extinction coefficients of NADPH at 340 nm for 50- and 100-μL volumes in the half-area plates were determined to be 1590 M^{-1} and 3170 M^{-1}, respectively, and 680 M^{-1} at 370 nm for a 50-μL volume. Initial velocity data were obtained at variable concentrations of acetoacetyl-CoA (0.40−10 mM) and changing-fixed concentrations of NADPH (50−1500 μM). The apparent kinetic constants of AcAc-ACP were obtained by varying the concentration of AcAc-ACP (20−100 μM) at a fixed concentration of NADPH (250 μM). Product inhibition patterns of $NADP^+$ and D,L-3-hydroxybutyryl-CoA vs both substrates were obtained with variable concentrations of either NADPH (50−250 μM) or AcAc-CoA (2.9−6 mM) at fixed concentrations of the other substrate, AcAc-CoA (5 mM) and NADPH (250 μM), respectively.

pH−Rate Profiles. A multicomponent buffer consisting of 66 mM MES, 34 mM DEA, 34 mM TEA, and 100 mM NaCl dissolved in Millipore-filtered water was used for the pH−rate studies. The buffer was adjusted to the desired pH by titrating with HCl or KOH (pH 5.5−9.5). This buffer system gives constant ionic strength (*I*) of 0.15 (*14*). Initial rates of the reaction catalyzed by KACPR at the stated pH values were measured by varying the concentration of one of the substrates while maintaining the other at a fixed, (near-) saturating level. The kinetic parameters *V* and *V*/*K* for acetoacetyl-CoA and NADPH were determined by varying the concentration of acetoacetyl-CoA between 0.08 and 10 mM at 500 μM of NADPH, and by varying the concentration of NADPH between 100 and 500 μM at a saturating concentration of AcAc-CoA (10 mM), respectively, and by fitting of the resulting data as described below.

Primary and α*-Secondary Deuterium and Solvent Kinetic Isotope Effects.* Primary deuterium kinetic isotope effects were determined via initial velocity kinetics at variable concentrations of [4*S*-^{1}H]- and [4*S*-^{2}H]NADPH (100−500 μM) and at saturating (5 mM) and subsaturating (1 mM) concentrations of acetoacetyl-CoA, or at variable concentrations of AcAc-CoA (0.15−5.0 mM) at 0.25 or 1.5 mM [4*S*-^{1}H]- and [4*S*-^{2}H]NADPH, at pH 7.6 (200 mM HEPES), 9.0 (200 mM bis-tris-propane), and 10 (200 mM CAPS) in 100 mM NaCl. α-Secondary deuterium isotope effects on *V* and $V/K_{AcAc-CoA}$ were determined at variable concentrations of acetoacetyl-CoA (0.150−5.0 mM) and at saturating (1.5 mM) concentrations of [4*R*-^{1}H]- and [4*R*-^{2}H]NADPH at pH 7.6 (200 mM HEPES), 9.0 (200 mM bis-tris-propane), and 10.0 (200 mM CAPS) in 100 mM NaCl. Solvent kinetic isotope effects for both substrates were measured at variable concentrations of AcAc-CoA (0.39−10 mM), and a fixed saturating concentration of NADPH (1.5 mM), and at variable concentrations of NADPH (0.05−1.5 mM) and a fixed, saturating concentration of acetoacetyl-CoA (5 mM) in 50 mM HEPES prepared in H_2O or 99.9% D_2O at pH(D) 7.5, 100 mM NaCl at 30 °C. Multiple isotope effects were measured by determination of the primary deuterium isotope effects in a buffer composed of 200 mM HEPES (pD 7.6) in D_2O.

Data Analysis. Kinetic data were fitted to the appropriate rate equations by using the nonlinear regression function of SigmaPlot 2000 (SPSS, Inc.). Initial velocity data at a single concentration of the fixed substrate were fitted to eq 1 to determine the kinetic parameters, *V* and *V*/*K*.

$$v = VA/(K + A) \quad (1)$$

Data for intersecting initial velocity patterns were fitted to eq 2, which conforms to a sequential kinetic mechanism. Data for competitive and noncompetitive inhibition were fitted to eqs 3 and 4, respectively. For eqs 1−4, *V* is the maximal velocity, *A* and *B* are substrate concentrations, *I* is inhibitor concentration, K_{ia} is the dissociation constant for A, K_a and K_b are Michaelis constants for substrates A and B, respectively, and K_{is} and K_{ii} are the slope and intercept inhibition constants, repsectively.

$$v = VAB/(K_{ia}K_b + K_aB + K_bA + AB) \quad (2)$$

$$v = VA/[K(1 + I/K_{is}) + A] \quad (3)$$

$$v = VA/[K(1 + I/K_{is}) + (1 + I/K_{ii})A] \quad (4)$$

Data for all pH profiles were fitted to eqs 5 and 6, in which *y* is the observed kinetic parameter *V*/*K* or *V*, *c* is the pH-independent value of *y*, *H* is the concentration of hydrogen ion, and K_a−K_d are either individual, apparent acid or base dissociation constants, or products and/or sums of dissociation and kinetic rate constants. The steady-state primary and

$$\log y = \log\{c/[1 + H/K_a + K_b/H]\} \quad (5)$$

$$\log y = \log\{[c(1 + K_a/H)]/[(1 + H/K_b + K_c/H)(1 + K_d/H)]\} \quad (6)$$

secondary deuterium and solvent kinetic isotope effects were determined by fitting the experimental initial rates at variable concentrations of one substrate (A) at fixed levels of the other (B) to eqs 7 and 8, where eq 7 describes the case where ^{D}V and $^{D}V/K_a$ are not equal, and eq 8 describes the case where ($^{D}V = {}^{D}V/K_a$). For eqs 7 and 8, *A* is the variable substrate,

$$\nu = VA/[K_a(1+ F_iE_{V/Ka}) + A(1 + F_iE_V)] \quad (7)$$

$$\nu = VA/[(K_a + A)(1 + F_iE_V)] \quad (8)$$

F_i is the fraction of deuterium label ($F_i = 0.0$ and 1.0 for hydrogen- and deuterium-containing NADPH or H_2O, respectively), $E_{V/Ka}$ is the isotope effect minus 1 on V/K_a, and E_V is the isotope effect minus 1 on *V*. For each case, the most appropriate fit was chosen according to a Student's *T*-test comparison in which the residuals from fits of comparable data sets of the light and heavy isotopes were used to determine if the higher order function is a statistically better fit.

Nomenclature. Isotope effects are expressed using the notation of Cleland, Northrop, and Cook (*15*, *16*). The nature of the isotope effects measured on the kinetic parameters *V*/*K* and *V* are notated as leading superscripts, with the variable substrate as the right subscript. For multiple isotope effects, the second isotope, which is at a fixed level in the measurement, is notated as a right subscript.

RESULTS AND DISCUSSION

Kinetic Mechanism of KACPR. The initial velocity pattern of AcAc-CoA vs NADPH was intersecting, indicative of a sequential kinetic mechanism, which upon fitting to eq 2 yielded values of $k_{cat} = 11 \pm 2\ s^{-1}$, $K_{NADPH} = 400 \pm 120\ \mu M$, $K_{AcAc-CoA} = 2200 \pm 670\ \mu M$, $k_{cat}/K_{NADPH} = 28 \pm 8\ mM^{-1}\ s^{-1}$, and $k_{cat}/K_{AcAc-CoA} = 5 \pm 2\ mM^{-1}\ s^{-1}$ (data not shown). Product inhibition patterns of $NADP^+$ vs NADPH, D,L-3-hydroxybutyryl-CoA vs NADPH, and D,L-3-hydroxybutyryl-CoA vs AcAc-CoA were all competitive, while that of $NADP^+$ vs AcAc-CoA was noncompetitive (Table 1). As all product inhibition patterns were competitive except the noncompetitive pattern observed for the plot of $NADP^+$ vs AcAc-CoA, these results are consistent with a random bi-bi kinetic mechanism for *S. pneumoniae* KAPCR, in which a dead-end E−AcAc-CoA−$NADP^+$ complex is formed (*17*). The initial velocity pattern of NADPH vs the physiological AcAc-ACP substrate was also intersecting, demonstrating a sequential mechanism ($k_{cat} = 18 \pm 1\ s^{-1}$, $K_{AcAc-ACP} = 23 \pm 5\ \mu M$, and $k_{cat}/K_{AcAc-ACP} = 800 \pm 180\ mM^{-1}\ s^{-1}$), however due to nonlinearity in the double-reciprocal plots (presumably arising either from positive cooperativity of AcAc-ACP binding or a steady-state random mechanism), further work with this substrate has not progressed (data not shown).

The ordered mechanism proposed by Price et al. (*11*) for *E. coli* KACPR in which NADPH must bind before AcAc-ACP is therefore not supported by these kinetic studies with the *S. pneumoniae* enzyme using AcAc-CoA as a substrate. Further studies of AcAc-ACP are required to understand whether the conformational changes inferred from structural studies are indeed reporting on an ordered kinetic mechanism for the ACP-substrate. The poorer substrate AcAc-CoA used in our studies may account for the random mechanism of substrate binding. Interestingly, the kinetic mechanisms of the related bacterial enoyl-ACP reductases from *Haemophilus influenzae* and *M. tuberculosis* using substrates bearing CoA rather than ACP substituents were also characterized as random bi-bi mechanisms, with observed kinetic isotope effects similar to what we present in this work (*18*, *19*), but the kinetic mechanism of enoyl-ACP reductase from *B. napus* was found to be ordered, with NADH binding before the CoA substrate (*20*). We expected that AcAc-CoA would prove a more useful substrate than AcAc-ACP for probing the kinetic and catalytic mechanisms of KACPR by use of kinetic isotope effects, as the poor substrate is expected to exhibit small commitment factors[2] (*15*, *16*).

Table 1: Product Inhibition Studies of *S. pneumoniae* β-Ketoacyl-ACP Reductase

varied substrate	product inhibitor	K_{is} (mM)	K_{ii} (mM)	inhibition type
NADPH	D,L-3-hydroxybutyryl-CoA	8 ± 1		C
β-AcAc-CoA	D,L-3-hydroxybutyryl-CoA	2.6 ± 0.4		C
NADPH	$NADP^+$	2.6 ± 0.3		C
β-AcAc-CoA	$NADP^+$	3.8 ± 2.5	1.9 ± 0.8	NC

The pH Dependence of KACPR Catalysis. The pH−rate profiles of the kinetic parameters $V/K_{NADPH}E_t$, $V/K_{AcAc-CoA}E_t$, and V/E_t as determined over the pH range of 5.5−9.5 are shown in Figure 1. Plots of log $V/K_{NADPH}E_t$, log $V/K_{AcAc-CoA}E_t$, and log V/E_t vs pH decreased at pH values <7.0 and >7.5, wherein none of the plots apparently conformed to classical "bell-shaped" curves, as described by eq 5, for which the curves in the plots would decrease below and above neutral pH with slopes of 1 and −1, respectively. Instead, the three pH−rate profiles were indicative of more complex functions, such as those described by eq 6, which would arise from (a) additional acid and base dissociation constants due to substrate or proton "stickiness" and/or (b) residual enzymatic activity of an unprotonated enzyme form at high pH (*17*).

Data from the three pH−rate profiles were fitted to both eqs 5 and 6, and the results of these fittings are shown in Table 2. Fitting of the data for log $V/K_{NADPH}E_t$ vs pH to eq 5 gave the poorer fit in terms of least-squares residual value, yielding apparent values $pK_a = 5.0 \pm 0.6$ and $pK_b = 8.8 \pm 0.2$. Use of eq 6 for these data improved the fitting in terms of residual least-squares, although not all of the apparent acid and base dissociation constants resulted in well-determined values, indicating that the data was not sufficiently robust or complete to allow fitting to this more complex function. Accordingly, fits of the plot of log $V/K_{NADPH}E_t$ vs pH could not be differentiated between eqs 5 and 6.

For the plot of the log $V/K_{AcAc-CoA}E_t$ vs pH, quality-of-fit of the data to either eq 5 or 6 was similar, the former of

[2] Equations for the isotope effects are of the form $^{D}V/K = [^{D}k + c_f + c_r{}^{D}K_{eq}]/[1 + c_f + c_r]$ and $^{D}V = [^{D}k + c_{Vf} + c_r{}^{D}K_{eq}]/[1 + c_{Vf} + c_r]$ in which c_f, c_{Vf}, and c_r are forward and reverse commitment factors, respectively. An external commitment factor is a component of the full commitment factor, and describes the partitioning of a substrate or product between progression through downstream isotope-sensitive enzymatic steps or its desorption from the enzyme (*15*, *16*).

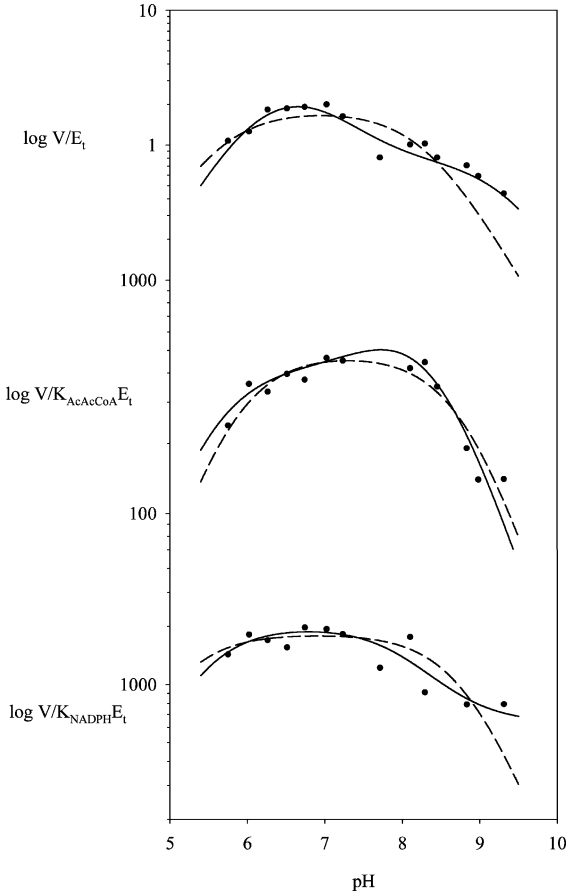

FIGURE 1: The pH Dependence of the KACPR kinetic parameters V/E_t and $V/K \cdot E_t$ for AcAc-CoA and NADPH. The curves were obtained from fits of the experiment data (points) at each pH to eqs 5 (dashed line) and 6 (solid line) for log $V/K_{NADPH}E_t$ vs pH, log $V/K_{AcAc-CoA}E_t$ vs pH, and log V/E_t vs pH.

which resulted in values of pK_a = 5.8 ± 0.1 and pK_b = 8.8 ± 0.1 which were nearly identical to those for the data of log $V/K_{NADP}E_t$ vs pH. For both substrates, the apparent acidic and basic dissociation constants of pK_a = 5.0−5.8 and pK_b = 8.8, respectively, likely represent an enzymatic acid and base found in the E−NADPH or E−AcAc-CoA binary complexes, or titratable groups on the substrates. The basic group of pK = 8.8 that must be protonated for catalysis is likely part of the tyrosine-lysine-serine catalytic triad recently reported for the *E. coli* enzyme by Price et al. (*8*). Although the pK of the hydroxyl group of the active-site tyrosine is in the range of ~10 in solution, reports of the pK of the conserved tyrosine found in all short-chain dehydrogenases have been in the range of 7.5−8.0 (*21*). The lowering of the pK of tyrosine from 10 to ~9 has been attributed to its interaction with the nearby conserved active site lysine residue and the ribose hydroxyl group of the nicotinamide substrate.

Apparent deviation of the data from a bell-shaped profile for the plot of log V/E_t vs pH suggested that deprotonation of the acidic group of apparent pK = 9 led to a diminished, rather than ablated, rate of catalysis by the E−NADPH−AcAc-CoA complex. Fitting of the data of V/E_t vs pH to both eqs 5 and 6 yielded more optimal fitting to the latter upon comparison of the least-squares residuals values, for which four dissociation constants were determined: pK_a = 7.6 ± 0.3, pK_b = 6.1 ± 0.2, pK_c = 7.0 ± 0.3, and pK_d = 9.4 ± 0.4. This better fitting of the data of V/E_t vs pH to eq 6 indicated that at high pH a form of the ternary complex E−NADPH−AcAc-CoA was able to progress through catalytic steps despite the apparent deprotonation of a key group of pK ~ 8.8 found in the binary enzyme−substrate complexes.

Primary and Secondary Deuterium and Solvent Kinetic Isotope Effects of KACPR. For enzymatic reactions evaluated in the direction of NAD(P)H oxidation, primary deuterium kinetic isotope effects typically range from 1 to 3 (*22*), while one expects to observe a normal α-secondary deuterium isotope effect ranging from values of 1.0 to the equilibrium isotope effect of [4-^{2}H]NAD(P)H reduction ($^{\alpha-D}K_{eq}$ = 1.13 (*23*)), in accord with a change in hybridization of the C-4 carbon from sp^3 to sp^2.

The primary and secondary kinetic isotope effects for KACPR are summarized in Table 3. Primary deuterium isotope effects were determined by comparison of the initial velocity data of [4*S*-^{1}H]- and [4*S*-^{2}H]NADPH (Figure 2), using both reduced nicotinamides and AcAc-CoA as variable substrates at a pH range of 7.6 to 10.0. Data fitted to both eqs 7 and 8 were found to best fit to eq 8, for which isotope effects obtained for all ^DV and $^DV/K$ values were equal (2.6) at pH 7.6.

By increasing the fixed level of NADPH from 0.25 mM to the near-saturating level of 1.5 mM, the value of $^D(V/K_{AcAc-CoA})_{H_2O}$ (2.3) was not suppressed to unity, but instead increased slightly (2.3 to 2.6; Table 3). This result indicates that the kinetic mechanism cannot be ordered with NADPH binding first, in agreement with the product inhibition studies described in this work (*15*). The large and equal values of 2.6 obtained for $^D(V/K_{NADPH})_{H_2O}$, and $^D(V/K_{AcAc-CoA})_{H_2O}$ at saturating levels of the fixed substrates suggest that (a) the mechanism is rapid-equilibrium random and (b) accordingly, the commitment factors for $^D(V/K_{NADPH})$, $^D(V/K_{AcAc-CoA})$, and ^DV are either negligible or very low.

Table 2: Data Fitting of pH−Rate Profiles of *S. pneumoniae* β-Ketoacyl-ACP Reductase[a]

kinetic parameter	eq fitted	residual (r^2)	fitted parameters				
			c[c]	pK_a	pK_b	pK_c	pK_d
log $V/K_{NADPH} \cdot E_t$	5	0.64	1830 ± 170	5.0 ± 0.6	8.8 ± 0.2	na[b]	na
	6	0.75	2000 ± 170	8.6 ± 0.6	5.3 ± 0.4	8.1 ± 0.4	>10 000
log $V/K_{AcAc-CoA} \cdot E_t$	5	0.88	480 ± 30	5.8 ± 0.1	8.8 ± 0.1	na	na
	6	0.93	420 ± 70	7.5 ± 0.9	5.5 ± 0.3	7.8 ± 1.1	8.4 ± 0.4
log V/E_t	5	0.75	1.8 ± 0.2	5.6 ± 0.3	8.3 ± 0.2	na	na
	6	0.93	3. 0± 0.75	7.6 ± 0.3	6.1 ± 0.2	7.0 ± 0.3	9.4 ± 0.4

[a] Results from fitting of the data found in Figure 1 to eqs 5 and 6 as described in Experimental Procedures. Error limits on those values were obtained from the fitting, which yielded residual values as shown. [b] Not applicable. [c] The c parameters are reported in arbitrary units.

Table 3: Primary, α-Secondary Deuterium, Solvent, and Multiple Kinetic Isotope Effects for *S. pneumoniae* KACPR[a]

parameter	pH(D) 7.6	pH 9.0	pH 10.0	fixed substrate, mM
$^{D}(V/K_{NADPH})_{H_2O}$	2.6 ± 0.4	2.1 ± 0.1	1.1 ± 0.03	5 mM AcAc-CoA
$^{D}(V/K_{AcAc-CoA})_{H_2O}$	2.6 ± 0.1	1.7 ± 0.1	0.91 ± 0.02	1.5 mM NADPH(D)
$^{D}(V/K_{AcAc-CoA})_{H_2O}$	2.3 ± 0.1[c]	nd[b]	nd	0.25 mM NADPH(D)
$^{D}(V_{NADPH})_{H_2O}$	2.6 ± 0.4	2.1 ± 0.1	1.1 ± 0.03	5 mM AcAc-CoA
$^{D}(V_{AcAc-CoA})_{H_2O}$	2.6 ± 0.1	1.7 ± 0.1	0.91 ± 0.02	1.5 mM NADPH(D)
$^{D}(V/K_{AcAc-CoA})_{D_2O}$	1.9 ± 0.1[c]	nd	nd	0.25 mM NADPH(D)
$^{D_2O}V/K_{NADPH}$	1.2 ± 0.1[c]	nd	nd	5 mM AcAc-CoA
$^{D_2O}V_{NADPH}$	1.2 ± 0.1[c]	nd	nd	5 mM AcAc-CoA
$^{D_2O}V/K_{AcAc-CoA}$	1.2 ± 0.1[c]	nd	nd	1.5 mM NADPH
$^{D_2O}V_{AcAc-CoA}$	1.2 ± 0.1[c]	nd	nd	1.5 mM NADPH
$^{\alpha-D}(V/K_{AcAc-CoA})_{H_2O}$	1.15 ± 0.02	1.00 ± 0.04	nd	1.5 mM NADPH(D)
$^{\alpha-D}(V_{AcAc-CoA})_{H_2O}$	1.15 ± 0.02	1.00 ± 0.04	nd	1.5 mM NADPH(D)

[a] Isotope effects were obtained by fitting of triplicate determinations of the initial rate data to eq 8, with experimental errors arising from the fitting. [b] Not determined. [c] Single determination

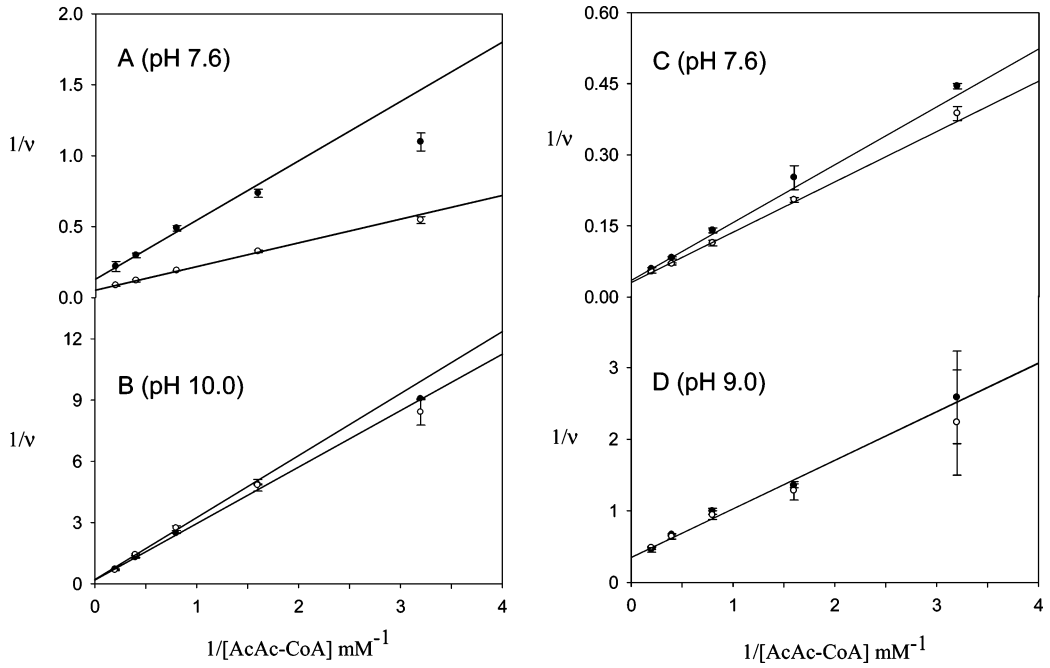

FIGURE 2: Double-reciprocal plots of the primary and α-secondary deuterium kinetic isotope effects for reduction of acetoacetyl-CoA by *S. pneumoniae* KACPR. Primary deuterium isotope effects varying acetoacetyl-CoA concentrations at pH 7.6 (A) and pH 10.0 (B) using 1.5 mM [4*S*-^{2}H]-NADPH (●) and 1.5 mM [4*S*-^{1}H]-NADPH (○). α-Secondary deuterium isotope effects varying acetoacetyl-CoA concentrations at pH 7.6 (C) and pH 9.0 (D) using 1.5 mM [4*R*-^{2}H]-NADPH (●) and 1.5 mM [4*R*-^{1}H]-NADPH (○). Experimental data are shown with lines obtained by fitting of the data to eq 8.

Similarly, the α-secondary deuterium isotope effects arising from substitution of the untransferred 4*R* hydrogen of NADPH with a deuterium was determined for V and $V/K_{AcAc-CoA}$ at 1.5 mM [4*R*-^{1}H]- and [4*R*-^{2}H]NADPH at pH 7.6 and 9.0 (Figure 2). Three initial-rate measurements were made at each concentration of AcAc-CoA, and the analysis of the differences in the measured initial velocities of [4*R*-^{1}H]- and [4*R*-^{2}H]NADPH by Student's *T*-test indicated that the observed rates for the two isotopes were significantly different from each other at all but the lowest concentration of the AcAc-CoA substrate at pH 7.6. Again, the resulting data were found to best fit to eq 8, such that $^{\alpha-D}(V/K_{AcAc-CoA})_{H_2O}$ and $^{\alpha-D}V_{H_2O}$ exhibited equal and significant values of 1.15 ± 0.02 for both parameters at pH 7.6. In summary, these large primary and secondary deuterium kinetic isotope effects suggest that the hydride-transfer reaction may be rate-limiting for KACPR, such that intrinsic isotope effects are nearly fully expressed, and are thereby indicative of small, if not absent, commitment factors.

Experimentally determined deuterium kinetic isotope effects are typically increased, often to their intrinsic values, when determined at pH values in which the catalytic activity is markedly attenuated due to changes in the protonation state of a critical catalytic residue. This is because catalysis becomes completely rate-limiting under these conditions, and the external catalytic commitment factors on the isotope effects are suppressed to near-zero values (*24*). Unexpectedly, at high pH, we observed a complete diminution, rather than augmentation, of all deuterium kinetic isotope effects to near-unity values at pH 9−10 (Figure 2 and Table 3). These findings suggest that, at high pH, either a critical proton-transfer step is greatly slowed, thereby becoming rate-limiting to catalysis and ablating the effect of the deuterium kinetic isotope effects, or, less likely, a postcatalytic step (a conformational change or product release step) becomes rate-limiting at high pH.

We investigated the impact of proton transfer on the rate-limiting step(s) of KACPR by the use of solvent kinetic

Scheme 2: pH-Dependence of the Random Bi-Bi Reaction of KACPR[a]

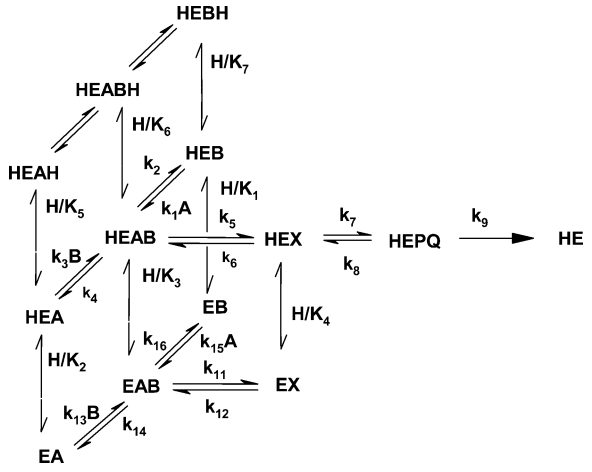

[a] The fixed substrate is saturating, and A is NADPH, B is AcAc-CoA, X is the reaction intermediate for the two stepwise mechanisms or would be the first enzyme−products complex for the concerted mechanism, and P and Q are the products 3-hydroxy-butyryl-CoA and $NADP^+$.

isotope effects. Minimally, one would anticipate a solvent kinetic isotope effect to accompany protonation of a putative enolate species generated during or via hydride transfer to the AcAc-CoA substrate from NADPH. In contrast to the deuterium isotope effects, the solvent kinetic isotope effects of KACPR at neutral values of pD were very modest, and again, all data were optimally fitted to eq 8 for which $^{D_2O}V/K_{NADPH} = {}^{D_2O}V/K_{AcAc-CoA} = {}^{D_2O}V = 1.2 \pm 0.1$ (Table 3). The notable differences in the primary deuterium ($\sim$2.6) and solvent (1.2) kinetic isotope effects suggested that hydride and proton transfer may occur on distinct reaction steps with different catalytic commitment factors, as discussed below. Assuming that the small solvent kinetic isotope effects arise solely from the protonation of the expected enolate intermediate of the KACPR reaction, measurement of both deuterium and solvent kinetic isotope effects on $V/K_{AcAc-CoA}$ afforded the opportunity for evaluation of the order of hydride- and proton-transfer steps in the mechanism of KACPR via multiple isotope effects (*25*). As shown in Table 3, the measured primary deuterium kinetic isotope effect on the parameter $V/K_{AcAc-CoA}$ decreased at neutral pH(D) when the value was measured in D_2O ($^{D}(V/K_{AcAc-CoA})_{H_2O} = 2.3 \pm 0.1$ and $^{D}(V/K_{AcAc-CoA})_{D_2O} = 1.9 \pm 0.1$), and as discussed below, this finding is consistent with hydride transfer and proton transfer occurring on distinct reaction steps.

Evaluation of the Chemical Mechanism of KACPR from pH−Rate Data and Kinetic Isotope Effects. Initial velocity, product inhibition data, and the pH−rate profiles were found to be consistent with the random bi-bi mechanism shown in Scheme 2. The complex (H)EAB represents the ternary

Scheme 3: Three Possible Chemical Mechanisms for KACPR, with the Steps that Could Express Intrinsic Isotope Effects Noted[a]

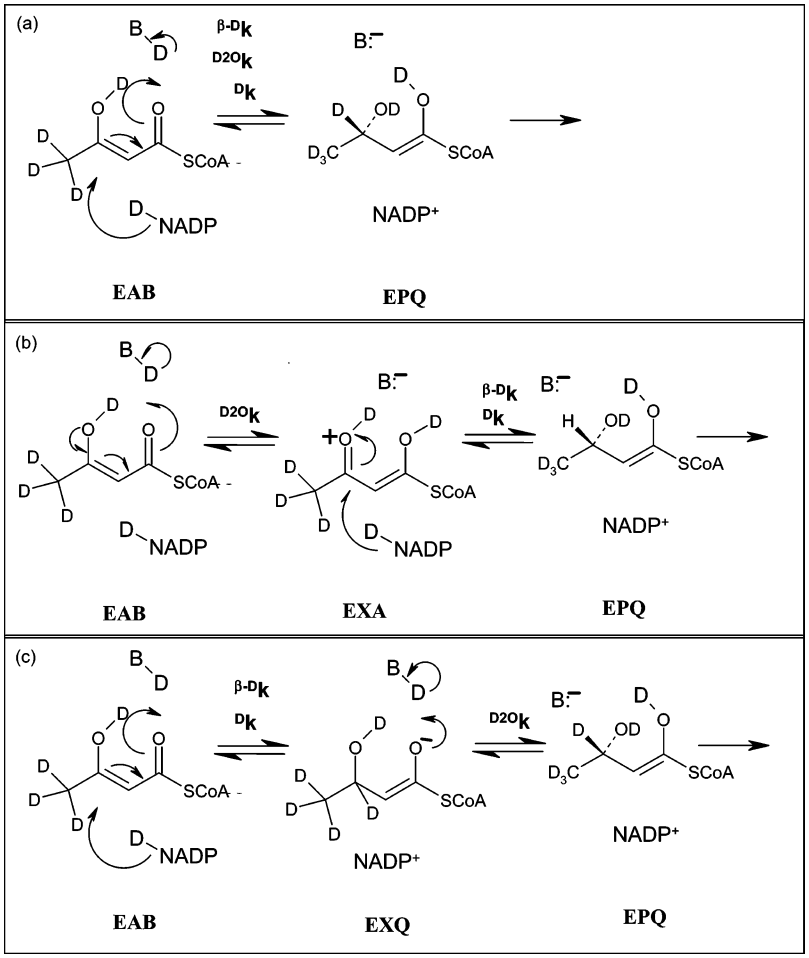

[a] (a) Concerted. (b) Stepwise: Protonation precedes hydride transfer. (c) Stepwise: Hydride transfer precedes protonation.

(H)E−NADPH−AcAc-CoA complex, while the (H)EX species represent an enzyme-bound reaction intermediate or reaction products. The acid dissociation constants K_5, K_6, and K_7 denote the observed apparent pK values of 5.0−5.8 measured in the plots of log V/K vs pH, and likewise, the base dissociation constants K_1, K_2, and K_3 reflect the apparent pK value of 9. The scheme includes a step in which the deprotonated species EAB is able to undergo catalysis at high pH, which is in accord with the data of log V vs pH wherein apparent catalysis is maintained at a pH which disfavors binding of the substrates. In the absence of the EX species, and under conditions in which k_{13}, k_{14}, k_{15}, and k_{16} are negligible, the plots of log V/K_{NADPH} and $V/K_{AcAc-CoA}$, respectively, are expected to comprise classic bell-shaped pH−rate profiles, and the same would be true for the plot of log V vs pH in the absence of the EAB to EX step.

For the general mechanism in Scheme 2, three chemical mechanisms could be envisioned for KACPR (Scheme 3): In the first (Scheme 3a), protonation of, and hydride transfer to, the presumed α,β-unsaturated, enolic thioester substrate[3] occur in a concerted fashion. Mechanisms b and c in Scheme 3 are stepwise in nature. In mechanism 3b, protonation of the thioester carbonyl by the enzymatic acid (in complex EXA) electrophilically activates the substrate prior to attack of the hydride from NADPH, as has been similarly shown for *E. coli* dihydrofolate reductase (*13*). In mechanism 3c, hydride transfer from NADPH to the β-carbon of the thioester generates an enolate intermediate in the EXQ complex, which is subsequently protonated by an enzymatic acid. Analysis of the isotope effects in this series of studies could allow discrimination of the three mechanisms in Scheme 3.

(a) Mechanistic Interpretation of the pH-Dependence of Deuterium Kinetic Isotope Effects. In order to interpret the kinetic isotope effects at variable pH, and therefore begin to address which chemical mechanism in Scheme 3 best describes KACPR catalysis, we derived kinetic expressions for the mechanism in Scheme 2. From application of the King−Altman method (*26*), and noting that $k_{11}K_3/k_5H = k_{12}K_4/k_6H$ and $k_{13}K_2/k_3H = k_{14}K_3/k_4H$, the following rate equations for the mechanism in Scheme 2 were obtained under conditions in which the fixed substrate is assumed to be at saturating concentration:

$$V/K_{NADPH}E_t = k_1k_5k_7k_9[1 + k_{11}K_3/k_5H][1 + k_{15}K_1/k_1H]/(1 + K_1/H + H/K_7)\{[1 + k_{16}K_3/k_2H][k_2k_6(k_8 + k_9)(1 + k_{11}K_3/k_5H) + k_2k_7k_9] + k_5k_7k_9(1 + k_{11}K_3/k_5H)\} \quad (9)$$

$$V/K_{AcAc-CoA}E_t = k_3k_5k_7k_9[1 + k_{11}K_3/k_5H][1 + k_{13}K_2/k_3H]/(1 + K_2/H + H/K_5)\{[1 + k_{14}K_3/k_4H][k_4k_6(k_8 + k_9)(1 + k_{11}K_3/k_5H) + k_4k_7k_9] + k_5k_7k_9(1 + k_{11}K_3/k_5H)\} \quad (10)$$

$$V/E_t = k_5k_7k_9(1 + k_{11}K_3/k_5H)/\{(1 + K_3/H + H/K_6)[k_6(k_8 + k_9)(1 + k_{11}K_3/k_5H) + k_7k_9] + k_5(k_8 + k_9)(1 + k_{11}K_3/k_5H)(1 + K_4/H) + k_5k_7(1 + k_{11}K_3/k_5H)\} \quad (11)$$

Equations 9−11 may be arranged in the forms of the two pH−rate equations (eqs 5−6) used to fit the experimental data in Figure 1, which are discriminated by the magnitudes of the ratios of the individual rate constants k_{15}/k_1, k_{16}/k_2, k_{13}/k_3, k_{14}/k_4, and k_{11}/k_5 shown in Scheme 2. For example, eqs 9−11 will reduce in form to the expression for a classical "bell-shaped" pH−rate profile (eq 5) when all of these ratios are approximately zero, whereas if k_{13}/k_3 and k_{14}/k_4 equal zero and k_{11}/k_5 represents a finite value in eq 10, data for the pH−rate profile of log $V/K_{AcAc-CoA}$ vs pH would be best fitted to eq 6. While data for log V/K_{NADPH} vs pH did not allow a definitive fit to either eq 5 or 6, data for log $V/K_{AcAc-CoA}$ vs pH fit to eq 6 slightly better than eq 5, such that we may conclude that the ratios k_{13}/k_3 and k_{14}/k_4 in Scheme 2 and eq 10 are negligible while k_{11}/k_5 is finite. Likewise, as data from the plot of log V/E_t vs pH were best fitted to eq 6, k_{11}/k_5 resultingly has a significant value and thereby there exists a kinetic contribution from the EAB to EX step. Accordingly, the pH−rate data are consistent with the mechanism in Scheme 2 in which the ternary complex E−NADPH−AcAc-CoA is capable of proceeding through a catalytic step (k_{11}) in its unprotonated form EAB as well as in the correctly protonated form HEAB (k_5).

Equations 9−11 were then transformed into expressions to describe the rate equations at neutral and high pH (eqs 12−17):

low pH

$$V/K_{NADPH}E_t = [k_1k_5k_7k_9]/[k_2k_6(k_8 + k_9) + k_2k_7k_9 + k_5k_7k_9] \quad (12)$$

$$V/K_{AcAc-CoA}E_t = [k_3k_5k_7k_9]/[k_4k_6(k_8 + k_9) + k_4k_7k_9 + k_5k_7k_9] \quad (13)$$

$$V/E_t = k_5k_7k_9/[(k_5 + k_6)(k_8 + k_9) + k_7(k_5 + k_9)] \quad (14)$$

high pH

$$V/K_{NADPH}E_t = (k_7k_9k_{11}k_{15})]/[k_{12}k_{16}(k_8 + k_9)(K_4/H)] \quad (15)$$

$$V/K_{AcAc-CoA}E_t = (k_7k_9k_{11}k_{13})/[k_{12}k_{14}(k_8 + k_9)(K_4/H)] \quad (16)$$

$$V/E_t = k_7k_9k_{11}/[(k_{11} + k_{12})(k_8 + k_9) + k_7k_{11}](K_4/H) \quad (17)$$

Expressions for the primary and secondary deuterium kinetic isotope effects may then be derived from eqs 12−17 at neutral and high pH. For the concerted mechanism in Scheme 3a, (H)EX would represent an enzyme−products complex, and accordingly, $k_8 = 0$. For the mechanism in Scheme 3b, the deuterium kinetic isotope effect is expressed on the k_7 step, with protonation of the substrate occurring on the k_5 step, while the opposite is true for the mechanism of Scheme 3c. From eqs 12−17, expressions for the primary and secondary deuterium kinetic isotope effects at neutral and high pH were derived for the three chemical mechanisms in Scheme 3 and are shown in Table 4.

For the concerted mechanism of Scheme 3a, one would intuitively expect that the deuterium kinetic isotope effects

[3] It is unknown which tautomer is recognized by KAPCR; we chose to represent the enolic-thio ester of AcAc-CoA as opposed to the keto form since Waterson and Hill (*1*) reported that it is the enol tautomer of AcAc-CoA that interacts with crotonase. Interpretations of kinetic data are identical regardless of the identity of the enzyme-bound tautomer.

Table 4: Expressions for Primary and Secondary Deuterium Kinetic Isotope Effects of KACPR for the Chemical Mechanisms in Schemes 2 and 3

kinetic parameter	I. Concerted Mechanism (3a) neutral pH	high pH
$^{D}(V/K_{NADPH})_{H_2O}$	$[^{D}k_5 + k_5/k_2 + (k_6/k_7)^{D}K_{eq5}]/[1 + k_5/k_2 + k_6/k_7]$	$[^{D}k_{11} + (k_{12}/k_7)^{D}K_{eq11}]/[1 + k_{12}/k_7]$
$^{D}(V/K_{AcAc-CoA})_{H_2O}$	$[^{D}k_5 + k_5/k_4 + (k_6/k_7)^{D}K_{eq5}]/[1 + k_5/k_4 + k_6/k_7]$	$[^{D}k_{11} + (k_{12}/k_7)^{D}K_{eq11}]/[1 + k_{12}/k_7]$
$^{D}V_{H_2O}$	$[^{D}k_5 + (k_5(k_7 + k_9)/k_7k_9) + (k_6/k_7)(^{D}K_{eq5})]/[1 + (k_5(k_7 + k_9)/k_7k_9) + k_6/k_7]$	$[^{D}k_{11} + (k_{12}/k_7)^{D}K_{eq11}]/[1 + k_{12}/k_7]$
$^{\alpha-D}(V/K_{AcAc-CoA})_{H_2O}$	$[^{\alpha-D}k_5 + k_5/k_4 + (k_6/k_7)^{\alpha-D}K_{eq5}]/[1 + k_5/k_4 + k_6/k_7]$	$[^{\alpha-D}k_{11} + (k_{12}/k_7)^{\alpha-D}K_{eq11}]/[1 + k_{12}/k_7]$
kinetic parameter	II. Stepwise Mechanism (3b): Protonation before Hydride Transfer neutral pH	high pH
$^{D}(V/K_{NADPH})_{H_2O}$	$[^{D}k_7 + (k_7/k_6)(1 + k_5/k_2) + (k_8/k_9)^{D}K_{eq7}]/[1 + (k_7/k_6)(1 + k_5/k_2) + k_8/k_9]$	$[^{D}k_7 + k_7/k_{12} + (k_8/k_9)^{D}K_{eq7}]/[1 + k_7/k_{12} + k_8/k_9]$
$^{D}(V/K_{AcAc-CoA})_{H_2O}$	$[^{D}k_7 + (k_7/k_6)(1 + k_5/k_4) + (k_8/k_9)^{D}K_{eq7}]/[1 + (k_7/k_6)(1 + k_5/k_4) + k_8/k_9]$	$[^{D}k_7 + k_7/k_{12} + (k_8/k_9)^{D}K_{eq7}]/[1 + k_7/k_{12} + k_8/k_9]$
$^{D}V_{H_2O}$	$[^{D}k_7 + (k_7(1 + k_5/k_9)/(k_5 + k_6) + (k_8/k_9)^{D}K_{eq7}]/[1 + (k_7(1 + k_5/k_9)/(k_5 + k_6) + k_8/k_9]$	$[^{D}k_7 + k_7/k_{12} + k_8/k_9{}^{D}K_{eq7}]/[1 + k_7/k_{12} + k_8/k_9]$
$^{\alpha-D}(V/K_{AcAc-CoA})_{H_2O}$	$[^{\alpha-D}k_7 + (k_7/k_6)(1 + k_5/k_4) + (k_8/k_9)^{\alpha-D}K_{eq7}]/[1 + (k_7/k_6)(1 + k_5/k_4) + k_8/k_9]$	$[^{\alpha-D}k_7 + k_7/k_{12} + (k_8/k_9)^{\alpha-D}K_{eq7}]/[1 + k_7/k_{12} + k_8/k_9]$
kinetic parameter	III. Stepwise Mechanism (3c): Hydride Transfer before Protonation neutral pH	high pH	eq
$^{D}(V/K_{NADPH})_{H_2O}$	$[^{D}k_5 + k_5/k_2 + (k_6/k_7)(1 + k_8/k_9)^{D}K_{eq5}]/[1 + k_5/k_2 + (k_6/k_7)(1 + k_8/k_9)]$	$[1 + (k_{12}k_2/k_7k_{11})(1 + (k_8/k_9))^{D}K_{eq11}]/[1 + (k_{12}k_2/k_7k_{11})(1 + (k_8/k_9))]$	18
$^{D}(V/K_{AcAc-CoA})_{H_2O}$	$[^{D}k_5 + k_5/k_4 + (k_6/k_7)^{D}K_{eq5}]/[1 + k_5/k_4 + (k_6/k_7)(1 + k_8/k_9)]$	$[1 + (k_{12}k_4/k_7k_{11})(1 + (k_8/k_9))^{D}K_{eq11}]/[1 + (k_{12}k_4/k_7k_{11})(1 + (k_8/k_9))]$	19
$^{D}V_{H_2O}$	$[^{D}k_5 + (k_5/k_7)[1 + k_7/k_9 + k_8/k_9] + (k_6/k_7)(1 + k_8/k_9)(^{D}K_{eq5})]/[1 + (k_5/k_7)[1 + k_7/k_9 + k_8/k_9] + k_8/k_9]$	$[1 + (k_{12}/k_{11})(k_8 + k_9)/[(k_8 + k_9) + 1]^{D}K_{eq11}]/[1 + (k_{12}/k_{11})(k_8 + k_9)/[(k_8 + k_9) + 1]$	20
$^{\alpha-D}(V/K_{AcAc-CoA})_{H_2O}$	$[^{\alpha-D}k_5 + k_5/k_4 + (k_6/k_7)(1 + k_8/k_9)^{\alpha-D}K_{eq5}]/[1 + k_5/k_4 + (k_6/k_7)(1 + k_8/k_9)]$	$[1 + (k_{12}k_4/k_7k_{11})(1 + (k_8/k_9))^{\alpha-D}K_{eq5}]/[1 + (k_{12}k_4/k_7k_{11})(1 + (k_8/k_9))]$	21

would be fully expressed on the kinetic parameters of V/K and V when proton-transfer becomes prohibitive at high pH in the EAB-to-EX step, since both proton and hydride transfer occur on the same rate-limiting step. The expressions for the kinetic isotope effects in Table 4 for the concerted mechanism bear this out, as the forward commitment factors k_5/k_2 and k_5/k_4 drop out of the expressions of $^{D}V/K_{NADPH}$ and $^{D}V/K_{AcAc-CoA}$, respectively, at high pH, which should result in increased experimental values of the isotope effects. The same is true for the ^{D}V and $^{\alpha-D}V/K_{AcAc-CoA}$ expressions. That the deuterium isotope effects diminish to unity at high pH suggests that the concerted mechanism is not operative for KACPR, unless a postcatalytic step, such as product release (k_7), becomes rate-limiting at high pH, and effectively raises the value of the reverse commitment factor k_{12}/k_7 to suppress the expression of the isotope effect. However, as the k_{12} step includes deprotonation of the hydroxyl product, one would expect this step to occur rapidly at both neutral and high pH.

For the stepwise mechanism in Scheme 3b, the unavailability of a proton at high pH slows the k_{11} step, which directly precedes hydride transfer (k_7), such that the ratios k_5/k_2, k_5/k_4, and k_5/k_9 are expected to be insignificant in the expressions for $^{D}V/K$ and ^{D}V, as is seen in Table 4. The loss of these forward commitment factors in the expressions in Table 4 at high pH is manifested in a reaction that is less "locked-in" prior to hydride transfer, and accordingly, maximal expression of the deuterium kinetic isotope effects is expected. However, as the opposite was observed, the mechanism of 3b would be at variance with the experimental results unless the unlikely case exists in which the k_{12} step (deprotonation of the carbonyl) was greatly slowed at high pH such that the k_7/k_{12} ratio becomes large compared to k_7/k_6. It is therefore improbable that protonation of the substrate precedes hydride transfer.

For the mechanism in Scheme 3c, the expected diminution at high pH of protonation of the enolate intermediate would drive the measured values of $^{D}V/K$, ^{D}V, and $^{\alpha-D}V/K$ to near-unity, as was observed. This is reflected in eqs 18−21 in Table 4, in which all four kinetic parameters will diminish to values between 1.0 and $^{D}K_{eq11}$ or $^{\alpha-D}K_{eq11}$ (0.84 and 1.13, respectively (*23*)). These findings are consistent with a stepwise mechanism for KACPR in which hydride transfer precedes proton transfer. These results are very similar to those observed for liver alcohol dehydrogenase in which the $^{D}V/K$ for the substrate cyclohexanol decreases to unity upon deprotonation of a catalytic enzymatic residue at high pH, which the authors attributed to a stepwise chemical mechanism in which hydride transfer preceded proton transfer (*27*).

(b) Mechanistic Interpretation of the Solvent and Multiple Kinetic Isotope Effects of KACPR. Measurement of both the deuterium and solvent kinetic isotope effects on $V/K_{AcAc-CoA}$ afforded the opportunity for evaluation of the mechanism of KACPR via multiple isotope effects (*25*). These studies could further enable the discrimination of the three chemical mechanisms depicted in Scheme 3, under conditions in which the small observed solvent kinetic isotope effects could reflect the expected proton-transfer step in the mechanism, rather than reflect any additional reaction steps, such as enzyme conformational changes. Expressions for the solvent and multiple kinetic isotope effects for KACPR are shown in Table 5.

The measured solvent isotope effects likely include an additional contribution from a β-deuterium secondary kinetic effect that would "report" on the hydride-transfer step. It is

Table 5: Expressions for the Solvent and Multiple Kinetic Isotope Effects for KACPR[a]

kinetic parameter	concerted (Scheme 3a)	protonation before hydride transfer (Scheme 3b)	hydride transfer before protonation (Scheme 3c)
$^{D_2O}(V/K_{AcAc-CoA})$	$[^{D_2O}k_5 + a + (1/b)^{D_2O}K_{eq5}]/[1 + a + 1/b]$	$[^{D_2O}k_5 + a + (1/b)(1 + c)^{D_2O}K_{eq5}]/[1 + a + (1/b)(1 + c)]$	$[^{D_2O}k_7 + (b)(1 + a) + c^{D_2O}K_{eq7}]/[1 + (b)(1 + a) + c]$
$^{D}(V/K_{AcAc-CoA})_{D_2O}$	$[^{D}k_5 + a/(^{D_2O}k_5{}^{\beta-D}k_5) + (1/b) \times (^{D_2O}K_{eq5}{}^{\beta-D}K_{eq5})/^{D_2O}k_5{}^{\beta-D}k_5)^{D}K_{eq5}]/[1 + a/(^{D_2O}k_5{}^{\beta-D}k_5) + (1/b) \times (^{D_2O}K_{eq5}{}^{\beta-D}K_{eq5})/^{D_2O}k_5{}^{\beta-D}k_5)]$	$[^{D}k_7 + b(^{D_2O}k_5/{}^{\beta-D}k_7{}^{D_2O}K_{eq5} \times (1 + a/^{D_2O}k_5) + c(^{\beta-D}K_{eq7}/{}^{\beta-D}k_7)^{D}K_{eq7}]/[1 + b(^{D_2O}k_5/{}^{\beta-D}k_7{}^{D_2}{}^{O}K_{eq5}) \times (1 + a/^{D_2O}k_5) + c(^{\beta-D}K_{eq7}/{}^{\beta-D}k_7)]$	$[^{D}k_5 + a/{}^{\beta-D}k_5 + (^{D_2O}k_7{}^{\beta-D}K_{eq5}/{}^{\beta-D}k_5b)(1 + c^{D_2O}K_{eq7}/{}^{D_2O}k_7)^{D}K_{eq5}]/[1 + a/{}^{\beta-D}k_5 + (^{D_2O}k_7{}^{\beta-D}K_{eq5}/{}^{\beta-D}k_5b) \times (1 + c^{D_2O}K_{eq7}/{}^{D_2O}k_7)]$

[a] Where $a = k_5/k_4$, $b = k_7/k_6$, $c = k_8/k_9$.

expected that each of the γ-carbon deuterons of the thioester substrate would contribute a maximal β-deuterium isotope effect of 0.955 per deuterium atom (*28*), such that values of $^{\beta-D}k$ would range from a minimal value of 1.0 to a maximal value of 0.87 (0.955^3) depending on the degree of change of hybridization of the γ-carbon deuterons in the transition state of the reaction**.** From the current study, one expects values for the intrinsic kinetic isotope effects to lie in the following ranges: $^{D_2O}k = 1.2-6.0$, $^{\beta-D}k = 0.87-1.0$ (the limiting value obtained from $^{\beta-D}K_{eq} = 0.87$), and $^{D_2O}K_{eq} = 1.84$ (calculated from published fractionation factors (*29*)). Accordingly, for the concerted mechanism, the forward commitment factor a (k_5/k_4; Table 5) would be reduced by a factor of $^{D_2O}k_5{}^{\beta-D}k_5$, or by 1.04−5.2, while the reverse commitment factor $1/b$ would be reduced by a factor of $^{D_2O}K_{eq5}{}^{\beta-D}K_{eq5}/^{D_2O}k_5{}^{\beta-D}k_5 = 0.75-3.75$. While one would then predict from this that $^{D}(V/K_{AcAc-CoA})_{D_2O} > {}^{D}(V/K_{AcAc-CoA})_{H_2O}$, the opposite was observed experimentally at pH(D) = 7.6 (Table 3). Along with the results of pH-dependence of the deuterium kinetic isotope effects, these results indicate that the concerted mechanism must be eliminated as a possibility for KACPR.

The identity of which of the two stepwise mechanisms is operative for KACPR may be further assessed by analysis of the expressions for the multiple kinetic isotope effects. It may be shown from the expressions in Table 5 that eq 22 holds for mechanism 3b and eq 23 for mechanism 3c (*30*).

$$(^{D}(V/K_{AcAc-CoA})_{H_2O} - 1)/(^{D}(V/K_{AcAc-CoA})_{D_2O} - 1) \sim {}^{D_2O}(V/K_{AcAc-CoA})/^{D_2O}K_{eq}{}^{\beta-D}k \quad (22)$$

$$(^{D}(V/K_{AcAc-CoA})_{H_2O} - {}^{D}K_{eq})/(^{D}(V/K_{AcAc-CoA})_{D_2O} - {}^{D}K_{eq}) \sim {}^{D_2O}(V/K_{AcAc-CoA})/^{\beta-D}k \quad (23)$$

Substitution of eqs 22 and 23 with experimental values of $^{D}(V/K_{AcAc-CoA})_{H_2O}$, $^{D}(V/K_{AcAc-CoA})_{D_2O}$, and $^{D_2O}(V/K_{AcAc-CoA})$ and literature values of $^{D_2O}K_{eq} = 1.84$ and $^{D}K_{eq} = 0.85$ and solving for $^{\beta-D}k$ yields eqs 24 and 25, respectively:

$$^{\beta-D}k \sim [(1.2 \pm 0.1)/1.84]/[(2.3 \pm 0.1 - 1)/(1.9 \pm 0.1 - 1)] = 0.45 \pm 0.1 \quad (24)$$

$$^{\beta-D}k \sim (1.2 \pm 0.1)/[(2.3 \pm 0.1 - 0.85)/(1.9 \pm 0.1 - 0.85)] = 0.9 \pm 0.2 \quad (25)$$

That the calculated value of $^{\beta-D}k \sim 0.9 \pm 0.2$ from eq 25 is in better agreement with the theoretical value of 0.87−1.0 than that obtained from eq 24 suggests that the multiple isotope effect data are more in accord with the stepwise mechanism of Scheme 3c than that of Scheme 3b. These results are also supported by the pH−rate dependence of the deuterium kinetic isotope effects. From both sets of isotope effects data we conclude that the chemical mechanism of KACPR is the stepwise mechanism in which hydride transfer precedes protonation, described in Scheme 3c. While alternative explanations exist for the effects of pH and D_2O on the deuterium isotope effects, the kinetic model here is self-consistent with the suggestion that the isotope effects are "reporting" on an expected proton-transfer step that becomes rate-limiting at high pH and that, in D_2O, contributes to the modest diminution of the observed deuterium kinetic isotope effect arising from contributions both from proton transfer on a distinct reaction step and from a secondary β-deuterium isotope effect occurring on the same step as hydride transfer. Despite the potential ambiguities of using solvent kinetic isotope effects to report on a single proton-transfer step in multistep enzymatic catalysis, in an approach similar to ours, Weiss et al. (1987) successfully utilized D_2O as the "second isotope" in a multiple-isotope effects study to rule out a concerted reaction mechanism for mammalian adenosine deaminase (*31*).

Estimates of the Intrinsic Primary and Secondary Kinetics Isotope Effects. Numerical analysis of the expressions for the kinetic isotope effects in Tables 4 and 5 could allow estimates of the intrinsic kinetic isotope effects ^{D}k, $^{\alpha-D}k$, and possibly ^{D_2O}k. It is clear that the identical values of 2.6 obtained for $^{D}(V/K_{NADPH})_{H_2O}$, $^{D}(V/K_{AcAc-CoA})_{H_2O}$, and $^{D}V_{H_2O}$ demand that commitment factors k_5/k_2, k_5/k_4, $(k_6/k_7)(1 + k_8/k_9)$, and $(k_5/k_7)[1/k_9 + (1 + k_8/k_9)]$ (Table 4) be either finite and identical or near-zero in value as would be the case wherein $k_5 \ll k_4$ and k_2, and $k_6 \ll k_7$. From this we will assume that the forward commitment factors for all of these isotope effects are equal. Normally the availability of as many experimental isotope effects as represented by the equations in Table 4 would afford the opportunity for exact solutions of the unknown kinetic parameters ^{D}k, $^{\alpha-D}k$, and the four commitment factors, with estimates of $^{D}K_{eq}$ and $^{\alpha-D}K_{eq}$ from literature values. However, since the experimental values for the expressions in Table 4 were identical (2.6) or 1.0, the simultaneous solutions of these parameters were not well-conditioned and gave inappropriate values. However the pH-dependence of $^{D}V/K_{AcAc-CoA}$ allows a calculation of the ratio of the reverse/forward commitment factors for that substrate. From Table 3, the value of $^{D}V/K_{AcAc-CoA} = 0.91$ at pH 10.0 was similar to the expected values of $^{D}K_{eq} = 0.85$ (for secondary alcohols (*23*)). From eq 19 (Table 4), where $^{D}K_{eq11} = 0.85$, the ratio of the reverse and forward commitment factors for AcAc-CoA may be solved from $(1 - {}^{D}V/K_{AcAc-CoA})/(^{D}V/K_{AcAc-CoA} - {}^{D}K_{eq}) = (1-0.91 \pm 0.01)/$

Table 6: Estimates of Intrinsic Primary and Secondary Deuterium Kinetic Isotope Effects of KACPR[a]

calcd intrinsic isotope effects			selected values of commitment factors			
$^{D}k_5$	$^{\alpha-D}k_5$	$^{D_2O}k_7$	k_5/k_4	$k_6/k_7(1 + k_8/k_9)$	k_6/k_7	k_8/k_9
2.60	1.15	200	0.0	0.0	0.0	0.0
2.63	1.15	21	0.007	0.01	0.01	0.0
2.66	1.15	11	0.013	0.02	0.02	0.0
2.68	1.16	8.0	0.02	0.03	0.03	0.0
2.74	1.16	5.3	0.033	0.05	0.05	0.0
2.88	1.17	3.3	0.067	0.1	0.1	0.0
3.02	1.17	2.67	0.100	0.15	0.01	0.0
4.71	1.24	1.60	0.500	0.75	0.01	0.0
6.83	1.33	1.47	1.000	1.5	0.01	0.0

[a] Intrinsic isotope effects were calculated from rearrangements of expressions found in Tables 3 and 4; for example, $^{D}k_5 = {}^{D}(V/K)[1 + k_5/k_4 + k_6/k_7(1 + k_8/k_9)] - [(k_5/k_4 + k_6/k_7(1 + (k_8/k_9)^{D}K_{eq5})]$. $^{D}(V/K)$ was the experimental result from Table 3, selected values of k_6/k_7 and k_8/k_9 were 0−0.1 and 0.0, respectively, and was calculated as $1.5(k_6/k_7)(1 + k_8/k_9)$. The following literature values of the equilibrium isotope effects were used: $^{D}K_{eq5} = 0.85$, $^{\alpha-D}K_{eq5} = 1.13$, $^{D_2O}K_{eq7} = 1.84$ (*23*, *29*). Recalculation of these experimental values ($^{D}(V/K)$, $^{\alpha-D}(V/K)$, ^{D}V, etc.) from the calculated intrinsic isotope effects and the selected commitment factors rendered values that agreed with experimental results obtained at both high and low pH within ±0.1.

$(0.91 \pm 0.01-0.85) = (k_{12}k_4/k_7k_{11})(1 + (k_8/k_9)) = (k_{12}k_4/k_7k_5)(1 + (k_8/k_9)) = 1.5 \pm 0.9$. Use of this calculated ratio of commitment factors then simplifies estimates of the intrinsic isotope effects as discussed below.

From the experimental results, one would expect that meaningful ranges of values of the intrinsic isotope effects for "semiclassical" behavior would be $^{D}k = 2.6-6.0$, $^{\alpha-D}k = 1.0-1.13$, and $^{D_2O}k = 1.2-6.0$. Accordingly, we calculated "candidate" values of the intrinsic kinetic isotope effects within these ranges by solving the expressions in Table 4 for the intrinsic isotope effects with reasonable, chosen values of the commitment factors and with literature values of $^{D}K_{eq} = 0.85$ and $^{\alpha-D}K_{eq} = 1.13$ (*23*), seeking the best match of the calculated values of $^{D}(V/K_{AcAc-CoA})$, $^{\alpha-D}(V/K_{AcAc-CoA})$, and ^{D}V with the experimentally determined ones in Table 3. These calculations, summarized in Table 6, demonstrate that in order to observe a meaningful solvent isotope effect, the commitment factors k_5/k_4 and $k_6/k_7(1 + k_8/k_9)$ cannot be zero. Calculations in Table 6 indicated that the most reasonable intrinsic isotope effects of $^{D}k = 2.7$, $^{D_2O}k = 5.3$, and $^{\alpha-D}k = 1.16$, which were mathematically compatible with the experimental values of $^{D}(V/K_{AcAc-CoA})_{H_2O}$, $^{\alpha-D}(V/K_{AcAc-CoA})_{H_2O}$, and $^{D_2O}(V/K_{AcAc-CoA})$, occurred when the commitment factors equaled $k_5/k_4 = 0.033$, and $k_6/k_7(1 + k_8/k_9) = 0.05$, as other values tested were outside of the expected theoretical limits of the three intrinsic isotope effects under conditions of "semiclassical" behavior.

The estimated intrinsic value of $^{\alpha-D}k = 1.16$ indicates that the observed α-secondary isotope effect for KACPR represents the value of the equilibrium isotope effect, although it is in slight excess of the literature value of $^{\alpha-D}K_{eq} = 1.13$ for NAD(P)H/D reduction (*23*). Other precedents suggest the estimated $^{\alpha-D}k$ value of KACPR is an intrinsic one. Kurz and Frieden (*32*) reported values of $^{\alpha-D}k = 1.14-1.16$ for the α-secondary deuterium isotope effect for the nonenzymatic reduction of 4-cyano-2,6-dinitrobenzenesulfonate by [4-^{2}H]NADH. Similarly, Sikorski et al. (*33*) have determined an intrinsic value of $^{\alpha-D}k = 1.13$ for NADPH for *E. coli* dihydrofolate reductase, although this result is attributed to nonclassical behavior. While larger intrinsic values of $^{\alpha-D}k$ (1.4−1.5) have been calculated from results with two dehydrogenases measuring [4-^{2}H]NAD reduction (owing in

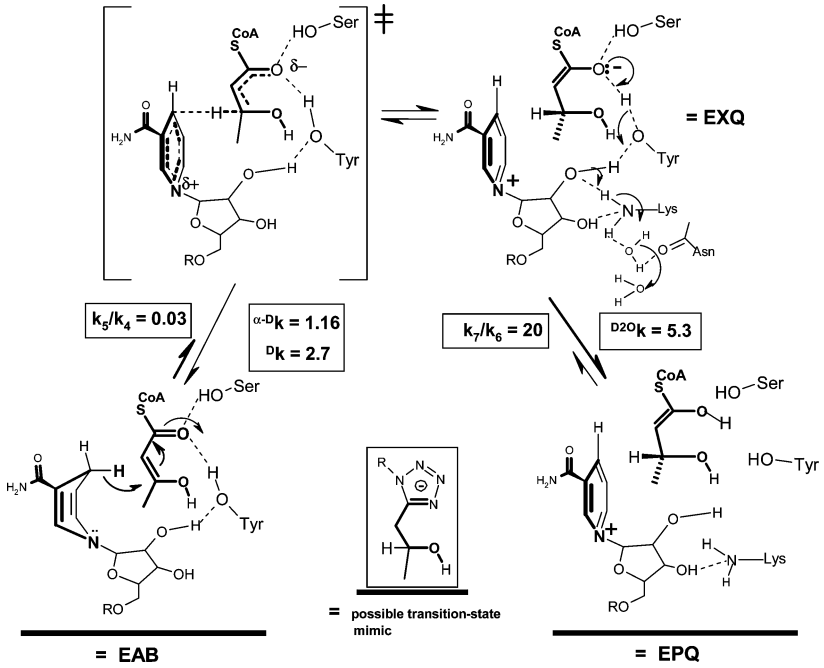

FIGURE 3: Schematic depiction of the proposed stepwise chemical mechanism of *S. pneumoniae* β-ketoacyl-ACP reductase. The values for the intrinsic isotope effects for the stepwise reaction of hydride transfer preceding proton transfer, $^{D}k = 2.7$, $^{D_2O}k = 5.3$, and $^{\alpha-D}k = 1.16$, and the commitment factors, $k_5/k_4 = 0.03$ and $k_7/k_6 = 20$, were derived from the work described in this manuscript. The possible transition-state mimic is a molecule conceptually derived from the proposed transition state in which the β-hydroxyl carbon develops sp^3-hybridization and a negative charge is created on the nascent, α-carbon enolate. The residues Ser, Tyr, Lys, and Asn represent active site amino acids serine 140, tyrosine 153, lysine 157, and asparagine 112 in *S. pneumoniae* β-ketoacyl-ACP reductase. The figure incorporates the proton network and relay system involving homologous Ser, Tyr, Lys, and Asn active site residues proposed by structural work for the *E. coli* and *B. napus* KACPR enzymes (*9*, *11*).

part to "coupled motion" of the hydride transferred from the alcohol substrate to NAD), values of $^{\alpha-D}k = 1.13-1.16$ represent the largest reported to date for [4-^{2}H]NAD(P)H oxidation (*25)*.

While we cannot conclude from available data that the α-secondary deuterium kinetic isotope effect of KACPR lacks a nonclassical component, and thereby should display a larger intrinsic value, the simplest interpretation of the observed primary and secondary deuterium isotope effects of KACPR is that they reflect intrinsic values, and that they are reporting on a late transition state in the hydride-transfer step. These results are similar to those of yeast formate dehydrogenase ($^{\alpha-D}k = 1.23$, $^{D}k = 2.8$ (*23*, *30*)) and *E. coli* dihydrofolate reductase at high pH ($^{\alpha-D}k = 1.13$ (*33*); $^{D}k = 3$ (*13*)). Both sets of isotope effects were likewise thought to reflect a late transition state in these enzymatic reactions.

Summary of the Chemical Mechanism of KACPR and the Rational Design of Inhibitors. We conclude that the chemical mechanism of the *S. pneumoniae* KACPR proceeds via a stepwise chemical mechanism in which hydride transfer from NADPH to the AcAc-CoA substrate precedes protonation of the enzyme-bound adduct. The catalytic step involving hydride transfer is a "poorly" committed step ($k_5/k_4 = 0.033$), which gives rise to virtually complete expression of the primary and α-secondary kinetic isotope effects on the experimental kinetic parameters $^{D}(V/K)$ and $^{\alpha-D}(V/K)$, such that the kinetic mechanism is in effect rapid-equilibrium random. The estimated intrinsic values of $^{D}k = 2.7$ and $^{\alpha-D}k = 1.16$ suggest that the transition state for the hydride-transfer step is late, wherein the nicotinamide ring of NADPH assumes a nearly planar geometry and the β-keto carbon has attained nearly full sp^3-hybridization (Figure 3). The resulting enolate intermediate then rapidly "switches on" the proton relay system, giving rise to the highly committed proton-transfer step to form product ($k_7/k_6 = 20$), such that the expression of a large intrinsic value of $^{D_2O}k_7 = 5.3$ is attentuated in the experimental parameters of $^{D_2O}(V/K)$ and ^{D_2O}V. This large estimate of $^{D_2O}k_7$ would be consistent with a reaction step involving multiple proton transfers.

Although KACPR is related to the other SDR reductase in the FAS pathway, enoyl-ACP reductase (ENR), the potent inhibitors of ENR, triclosan and isoniazid, have not been reported to inhibit KACPR. Modeling studies suggested that steric constraints may be the only factor preventing triclosan or isoniazid from binding to the KACPR−NADP$^+$complex; however, neither of these compounds contain obvious structural features of the proposed transition states of KACPR (*9*). Our studies contribute to the recommendation that high-throughput screening for identifying KACPR inhibitors should be carried out on the NADP$^+$ bound form of the enzyme, which, from this work, is the form of the enzyme most representative of the appropriate transition state of KACPR catalysis. Finally, elucidation of the transition states of the KACPR reaction may provide possible starting points for the rational design of inhibitors of KAPCR. The late transition state of the hydride-transfer step immediately suggests two exploitable structural features: the incipient sp^3-hybridization of the β-keto carbon and the developing negative charge on the nascent enolate. One could imagine from this that the replacement of the acetoacetyl substituent of AcAc-CoA, or its smaller analogue, with the β-hydroxypropyl tetrazole pictured in Figure 3 may contribute both of these transition-state components and thereby may render the core structure of an exceptionally potent inhibitor of bacterial KACPR.

ACKNOWLEDGMENT

We acknowledge Professor Paul Cook for helpful discussions, Anthony Choudhry, John Martin, and Howard Kallender for the provision of AcAc-ACP, and Brett Claffee for provision of the KACPR-cloned *E. coli* fermentation for purification of KACPR.

REFERENCES

1. Waterson, R. M., and Hill, R. L. (1972*)* Enoyl Coenzyme A Hydratase (Crotonase). Catalytic Properties of Crotonase and its Possible Regulatory Role In Fatty Acid Oxidation, *J. Biol. Chem. 247*, 5258−5265.
2. Campbell, J. W., and Cronan, J. E., Jr. (2001) Bacterial Fatty acid Biosynthesis: Targets For Antibacterial Drug Discovery, *Annu. Rev. Microbiol. 55*, 305−332.
3. White, S. W., Zheng, J., Zhang, Y. M., and Rock, C. O. (2005) The Structural Biology Of Type II Fatty Acid Biosynthesis, *Annu. Rev. Biochem. 74*, 791−831.
4. Chen, Z., Jiang, J. C., Lin, Z. G., Lee, W. R., Baker, M. E., and Chang, S. H. (1993) Site-specific mutagenesis of *Drosophila* alcohol dehydrogenase: Evidence for involvement of tyrosine-152 and lysine-156 in catalysis, *Biochemistry 32*, 3342−3346.
5. Zheng, R. and Blanchard, J. S. (2000) Identification of Active Site Residues in *E. coli* Ketopantoate Reductase by Mutagenesis and Chemical Rescue, *Biochemistry 39*, 16244−16251.
6. Zhang, Y. M., and Rock, C. O. (2004*)* Evaluation of Epigallocatechin Gallate and Related Plant Polyphenols as Inhibitors of the FabG and FabI Reductases of Bacterial Type II Fatty-acid Synthase, *J. Biol. Chem. 279*, 30994−31001.
7. Opperman, U., Filling, C., Hult, M., Shafqat, N., Wu, X., Lindh, M., Shafqat, J., Nordling, E., Kallberg, Y., Persson, B., and Jornvall, H. (2003) Short-chain dehydrogenases/reductases (SDR): the 2002 update, *Chem.-Biol. Interact. 143*−*144*, 247−253.
8. Price, A. C., Zhang, Y.-M., Rock, C. O., and White, S. W. (2001) Structure of β-Ketoacyl-[acyl carrier protein] Reductase from *Escherichia coli*: Negative Cooperativity and Its Structural Basis, *Biochemistry 40*, 12772−12781.
9. Fisher, M., Kroon, J. T. M., Martindale, W., Stuitje, A. R., Slabas, A. R., and Rafferty, J. B. (2000*)* The X-ray structure of *Brassica napus* β-keto acyl carrier protein reductase and its implications for substrate binding and catalysis, *Structure 8*, 339−347.
10. Cohen-Gonsaud, M., Ducasse, S., Hoh, F., Zerbib, D., Labesse, G., and Quemard, A. (2002) Crystal Structure of MabA from *Mycobacterium tuberculosis*, a Reductase involved in Long-chain Fatty Acid Biosynthesis, *J. Mol. Biol. 320*, 249−261.
11. Price, A. C., Zhang, Y. M., Rock, C. O., and White, S. W. (2004) Cofactor-Induced Conformational Rearrangements Establish a Catalytically Competent Active Site and a Proton Relay Conduit in FabG, *Structure 12*, 417−428.
12. Orr, G. A., and Blanchard, J. S. (1984) High-performance ion-exchange separation of oxidized and reduced nicotinamide adenine dinucleotides, *Anal. Biochem. 142*, 232−234.
13. Morrison, J. F., and Stone, S. R. (1988) Mechanism of the reaction catalyzed by dihydrofolate reductase from *Escherichia coli*: pH and deuterium isotope effects with NADPH as the variable substrate, *Biochemistry 27*, 5499−5506.
14. Ellis, K. J., and Morrison, J. F. (1982) Buffers of constant ionic strength for studying pH-dependent processes, *Methods Enzymol. 87*, 405−426.
15. Cook, P. F., and Cleland, W. W (1981) Mechanistic Deductions from Isotope Effects in Multireactant Enzyme Mechanisms, *Biochemistry 20*, 1790−1796.
16. Northrop, D. B. (1977) Determining the Absolute Magnitude of Hydrogen Isotope Effects, in *Isotope Effects on Enzyme-Catalyzed Reactions* (Cleland, W. W., O'Leary, M. H & Northrop, D. B. Eds.,) pp 122−152, University Park Press, Baltimore, MD.
17. Cleland W. W. (1977) Determining the chemical mechanisms of enzyme-catalyzed reactions by kinetic studies, *Adv. Enzymol. Relat. Areas Mol. Biol. 45*, 273−387.

18. Parikh, S., Moynihan, D. P., Xiao, G., and Tonge, P. J. (1999) Roles of Tyrosine 158 and Lysine 165 in the Catalytic Mechanism of InhA, the Enoyl-ACP Reductase from *Mycobacterium tuberculosis*, *Biochemistry 38*, 13623−13634.
19. Marcinkeviciene, J., Jiang, W., Kopcho, L. M., Locke, Y. L., and Copeland, R. A. (2001) Enoyl-ACP Reductase (FabI) of *Haemophilus influenzae*: Steady-State Kinetic Mechanism and Inhibition by Triclosan and Hexachlorophene, *Arch. Biochem. Biophys. 390*, 101−108.
20. Fawcett, T., Copse, C. L., Simon, J. W., and Slabas, A. R. (2000) Kinetic mechanism of NADH-enoyl-ACP reductase from *Brassica napus*, *FEBS Lett. 484*, 65−68.
21. Filling, C., Berndt, K. D., Benach, J., Knapp, S., Prozorovski, T., Nordling, E., Ladenstein, R., Jornvall, H. and Oppermann, U. (2002) Critical Residues for Structure and Catalysis in Short-chain Dehydrogenases/Reductases, *J. Biol. Chem. 277*, 25677−25684.
22. Cook, P. F. (1990) Kinetic and Regulatory Mechanisms of Enzymes from Isotope Effects, in *Enzyme Mechanisms from Isotope Effects* (Cook, P. F., Ed.) pp 203−228, CRC Press, Boca Raton, FL.
23. Cook, P. F., Blanchard, J. S., and Cleland, W. W. (1980) Primary and secondary deuterium isotope effects on equilibrium constants for enzyme-catalyzed reactions, *Biochemistry 19*, 4853−4858.
24. Cook, P. F., and Cleland, W. W. (1981) pH Variation of isotope effects in enzyme-catalyzed reactions. 1. Isotope- and pH-dependent steps the same, *Biochemistry 20*, 1797−1804.
25. Hermes, J. D., Roeske, C. A, O'Leary, M. H., and Cleland, W. W. (1982) Use of multiple isotope effects to determine enzyme mechanisms and intrinsic isotope effects. Malic enzyme and glucose 6-phosphate dehydrogenase, *Biochemistry 21*, 5106−5114.
26. King E. L., and Altman, C. (1956) A Schematic Method of Deriving the Rate Laws for Enzyme-Catalyzed Reactions, *J. Phys. Chem. 60*, 1375−1378.
27. Cook, P. F., and Cleland, W. W. (1981) pH Variation of isotope effects in enzyme-catalyzed reactions. 2. Isotope-dependent step not pH dependent. Kinetic mechanism of alcohol dehydrogenase, *Biochemistry 20*, 1805−1816.
28. Geneste, P., Lamaty, G., and Roque, J. P. (1971) Reactions d'addition nucléophile sur les cétones: Addition de l'ion sulfite: mise en évidence de l'hyperconjugaison Par la mésure de l'éffet isotopique sécondaire du deuterium, *Tetrahedron 27*, 5539−5559.
29. Quinn, D. M., and Sutton, L. D. (1991) Theoretical Basis and Mechanistic Utility of Solvent Isotope Effects, in *Enzyme Mechanisms from Isotope Effects* (Cook, P. F., Ed.), pp 73−126, CRC Press, Boca Raton, FL.
30. Hermes, J. D., Morrical, S. W., O'Leary, M. H., and Cleland, W. W. (1984) Variation of transition-state structure as a function of the nucleotide in reactions catalyzed by dehydrogenases. 2. Formate dehydrogenase, *Biochemistry 23*, 5479−5488.
31. Weiss, P. M, Cook, P. F., Hermes, J. D., and Cleland, W. W. (1987) Evidence from nitrogen-15 and solvent deuterium isotope effects on the chemical mechanism of adenosine deaminase, *Biochemistry 26*, 7378−7384.
32. Kurz, L. C., and Friedan, C. (1980) Anomalous Equilibrium and Kinetic a-Deuterium Secondary Isotope Effects Accompanying Hydride Transfer from Reduced Nicotinamide Adenine Dinucleotide, *J. Am. Chem Soc. 102*, 4198−4203.
33. Sikorski, R. S., Wang, L., Markham, K. A., Rajagopalan, P. T. R., Benkovic, S. J., and Kohen, A. (2004) Tunneling and Coupled Motion in the *Eschericia coli* Dihydrofolate Reductase Catalysis, *J. Am. Chem. Soc. 126*, 4778−4779.

BI050947J